

## Geometrical Uniformity of Plastic Coatings on Optical Fibers

By H. M. PRESBY

(Manuscript received May 14, 1976)

*The concentricity and uniformity of nearly concentric transparent plastic coatings extruded onto optical fibers are determined by a sensitive, nondestructive optical technique. The method is based on the location of unique fringes in the backscattered light arising from a beam that is incident at right angles to the fiber's axis. Results from both uniform and distorted coatings are shown, and instrumentation suitable for on-line coating diagnosis and correction is presented.*

### I. INTRODUCTION

The use of plastic coatings in optical-fiber technology is multifaceted. The refractive index of many polymer materials is less than that of fused silica, enabling them to be used directly as the cladding for fused silica cores.<sup>1-3</sup> The resulting waveguides, suitable for many communication applications,<sup>4,5</sup> are relatively easy to fabricate, possess low loss and large numerical aperture, and are LED-compatible.

Plastic coatings are also applied as an overcoat to glass-clad optical fibers. They reduce microbending loss,<sup>6,7</sup> maintain the pristine strength of the fibers,<sup>8</sup> and provide for abrasion and mechanical protection of the fibers during cable-manufacturing processes. In yet other applications, coatings have been proposed as a method of decreasing crosstalk between optical fibers<sup>9</sup> and as a way of improving the long-term stability of fibers in uncontrolled environments.

To be most effective in all of the above applications, the coating must be applied uniformly and concentrically around the fiber. This is a necessity for routine handling and splicing as well as for optimum strength and transmission characteristics.

The coatings are applied by various methods, and techniques have been proposed and implemented with varying degrees of success to aid in their concentric application. In general, micropositioning and microscopic observations are necessary to align the fiber at the start of each application<sup>5</sup> and only by preparing and microscopically

examining sections of the fiber after the run can the quality of the coating be assessed. In addition to being time consuming and destructive, microscopic examination may not detect certain problems, such as geometrical nonuniformities that can seriously impair the transmission characteristics of the fiber. More importantly, real-time information to enable the fabricator to make corrections, evaluate various applicators or stop the process completely, is not available as the coating is being applied.

We present here a sensitive new method for analyzing transparent coatings on optical fibers. The technique is optical in nature being based on the location of unique fringes in the backscattered light<sup>10</sup> arising from a beam that is incident at right angles to the fiber axis. As such, it is inherently nondestructive and noncontacting. Most importantly, it is capable of providing in-line information on coating concentricity and uniformity as the coating is being applied.

## II. MEASUREMENT THEORY

Consider the two rays of light, I and II in Fig. 1, incident upon a coated optical fiber. Let the index of refraction and the radius of the

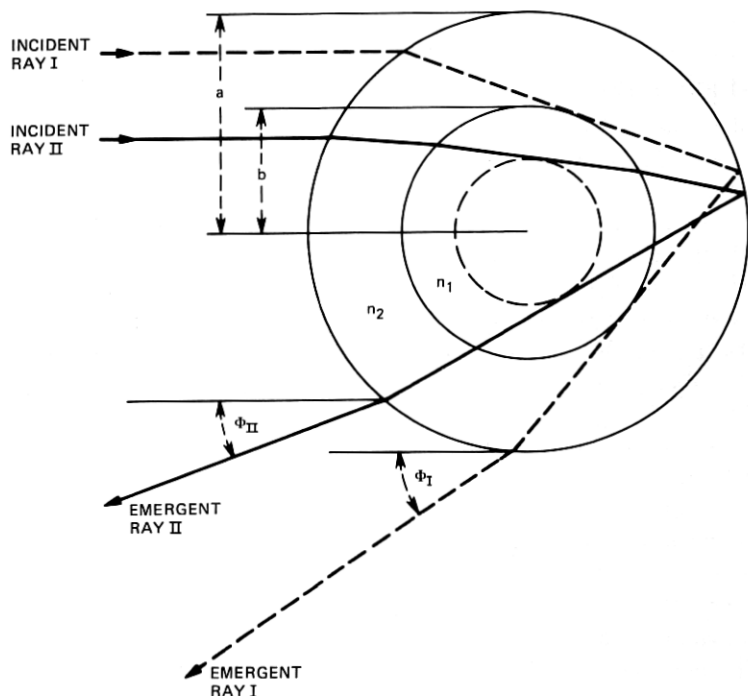


Fig. 1—Paths of rays of minimum deviation in a coated optical fiber. The situation is symmetric for rays incident upon the lower half of the fiber.

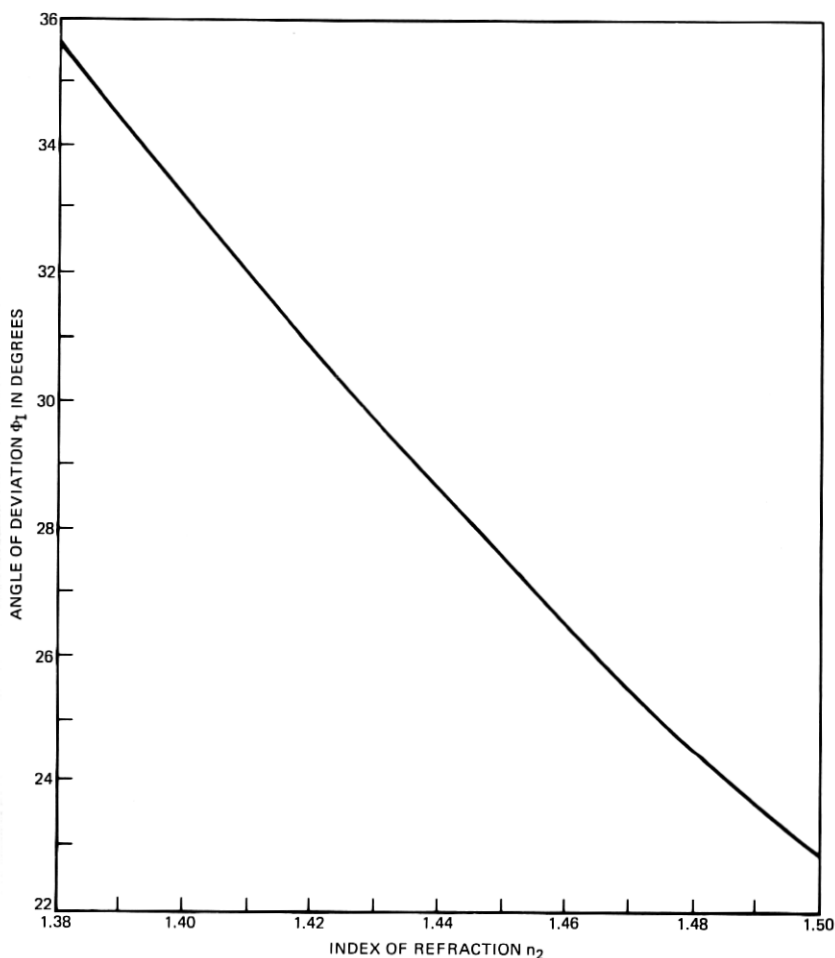


Fig. 2—Location of minimally deviated ray I as a function of the index of refraction of the coating  $n_2$ .

coating be  $n_2$  and  $a$ , respectively. For the purposes of the current analysis, the internal details of the fiber (indicated by the broken circle), which can be either an unclad, step-index, or graded-index variety, are neglected, and we let its index of refraction be  $n_1$  and its radius be  $b$ . We also neglect multiple internal reflections.

Ray I is refracted, traverses the coating, and is then reflected at the coating-air interface and exits making an angle of minimum deviation  $\phi_1$  with its incident direction given by<sup>10</sup>

$$\phi_1 = 4 \sin^{-1} \left[ \frac{2}{n_2 \sqrt{3}} \left( 1 - \frac{n_2^2}{4} \right)^{\frac{1}{2}} \right] - 2 \sin^{-1} \left[ \frac{2}{\sqrt{3}} \left( 1 - \frac{n_2}{4} \right)^{\frac{1}{2}} \right]. \quad (1)$$

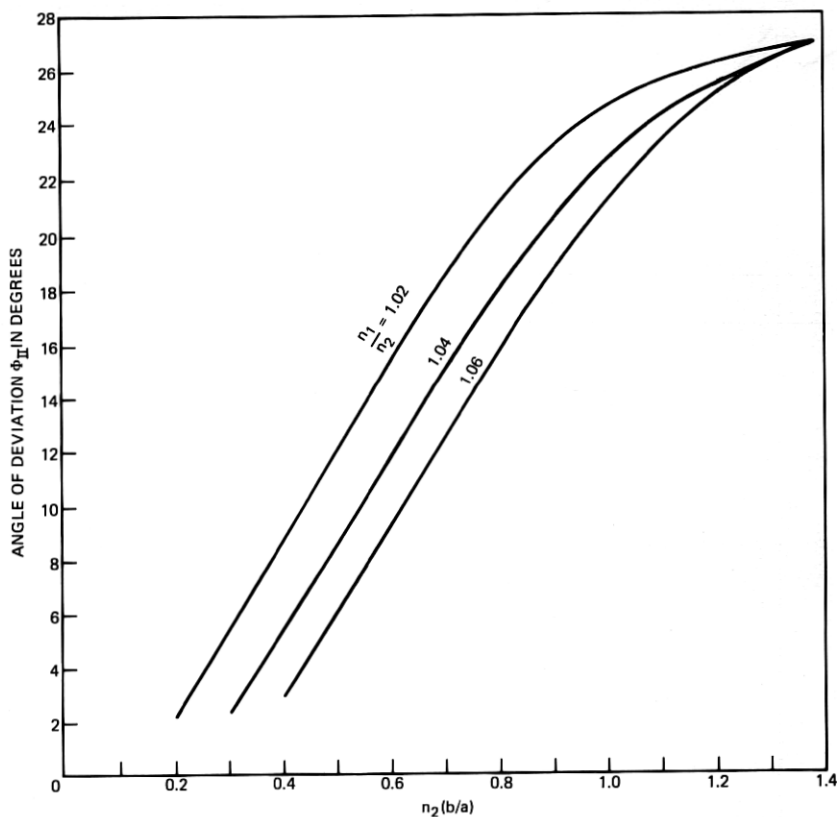


Fig. 3—Location of the minimally deviated ray II, as a function of  $n_2b/a$  for  $n_1/n_2 = 1.02, 1.04,$  and  $1.06$ .

A plot of  $\Phi_I$  versus  $n_2$  is given in Fig. 2. A maximum of intensity dependent only upon the refractive index of the coating,  $n_2$ , exists at this angle. Beyond  $\Phi_I$ , the backscattered pattern cuts off into a low level continuum.

Ray II, after being refracted by the coating, traverses the fiber, emerges into the coating, and is reflected by the coating-air interface. The ray then again enters the fiber and emerges into the coating and from there leaves the fiber, making an angle of minimum deviation  $\Phi_{II}$  with its incident direction.  $\Phi_{II}$  is a function of several angles and of  $n_1$  and  $n_2$ .<sup>11</sup>

Plots of  $\Phi_{II}$  determined by computer as a function of  $n_2b/a$  with  $n_1/n_2$  as a parameter are shown in Fig. 3 for  $n_1/n_2 = 1.02, 1.04,$  and  $1.06$ . For these calculations,  $n_1$  was held fixed at the fused-silica value of 1.457.

Figure 4 presents  $\Phi_{II}$  as a function of coating thickness ( $a - b$ ) for  $n_1 = 1.457$  and  $n_2 = 1.400$ . It is seen that a  $1\text{-}\mu\text{m}$  variation in thickness corresponds to an approximately  $0.1\text{-degree}$  shift in  $\Phi_{II}$ .

It is important to note that ray I does not see the fiber at all. For a given  $n_2$ , however, a critical fiber radius  $b_c$  (or alternatively, coating thickness) will exist beyond which ray I will no longer exist. This condition is given by<sup>11</sup>

$$b_c = a/n_2. \quad (2)$$

The disappearance of ray I is thus a very sensitive indication of a specific coating thickness. For example, if  $b = 50\ \mu\text{m}$ , a typical value, ray I will not be observed if the coating ( $n_2 = 1.4$ ) is less than  $20\text{-}\mu\text{m}$  thick. In general, the status of ray I is only an additional indicator, and coating-thickness measurements are based on the location of ray II. It is also important to note that distortions of the coating or fiber from the ideal circularity assumed here can have a significant effect on the location of  $\Phi_I$  and  $\Phi_{II}$ .<sup>12</sup>

### III. MEASUREMENT TECHNIQUE AND RESULTS

The experimental arrangement to observe the backscattered pattern is shown in Fig. 5.<sup>11</sup> Light from a cw *He-Ne* laser strikes plane mirror *M1* which reflects it to oscillating mirror *M2*. This serves to

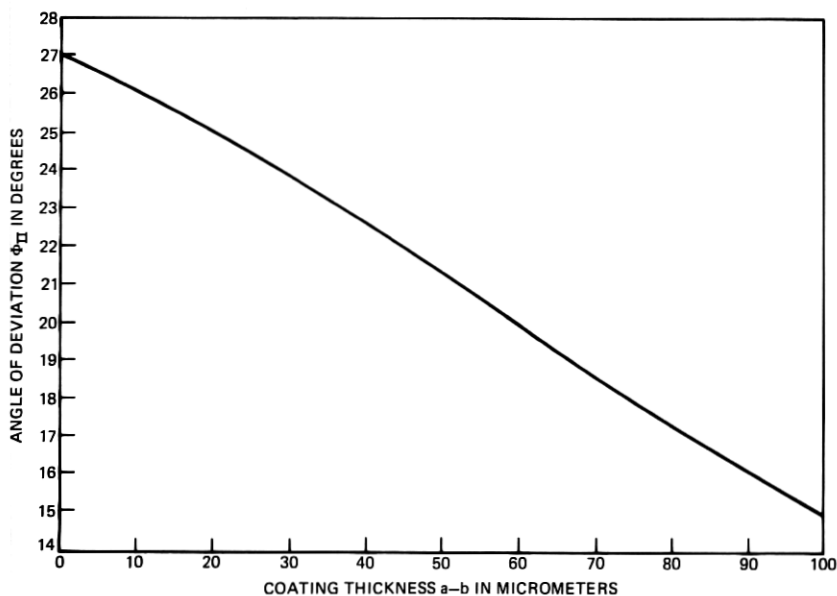


Fig. 4—Value of  $\Phi_{II}$  as a function of coating thickness  $a - b$  for a concentric and geometrically uniform fiber.

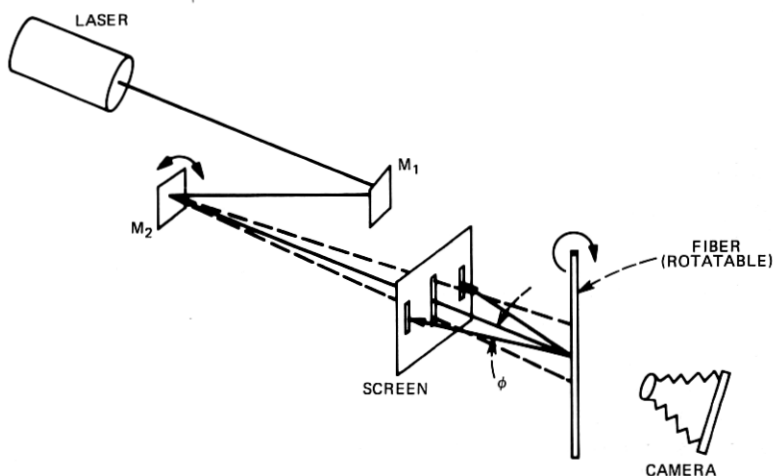


Fig. 5—Experimental arrangement to observe the backscattered patterns.

transform the approximately 1-mm circular beam into a line 1-mm wide, with length determined by the amplitude of oscillation, thus allowing for observations on an extended length of coated fiber, upon which the light impinges after passing through a slit in the observation screen. The fiber is held in a rotatable mount and the backscattered light falling on the screen is photographed with a  $4 \times 5$  framing camera. All of the results to be presented were obtained in this manner with stationary fibers.

A series of patterns, observed on the screen arising from a severely nonconcentric coated fiber, is shown in Fig. 6. The patterns are obtained as the fiber is rotated in 30-degree increments. The approximately  $150\text{-}\mu\text{m}$ -diameter glass fiber, also displayed in Fig. 6, is coated with a silicone resin which varies in thickness from a maximum of approximately  $85\ \mu\text{m}$  to a minimum of  $8\ \mu\text{m}$ . In this and all subsequent results, there is a one-to-one correspondence between a region in the backscattered pattern and a region in the approximately 65-mm illuminated length of fiber. The main fringes arising from rays I and II are labeled in the 0- to 150-degree orientations. The 0-degree origin of the rotational increments in this case was arbitrarily chosen to coincide with a maximum visibility of rays I and II. The light distribution exhibits large variations as the fiber is rotated due to the nonconcentricity of the coating. For example, in the 30-degree orientation, only one of the fringes corresponding to ray I appears; at 120 degrees, only the other one appears; and at 60 degrees both of them are absent. In all orientations, the fringes corresponding to rays II vary in location and in some positions in visibility. If observations of

the backscattered pattern were made for two mutually perpendicular orientations while such a fiber was being pulled, it would be readily ascertained by the visual appearance of the light distribution alone that the coating was nonconcentric and corrective measures could be taken.

An optical fiber with a somewhat improved coating concentricity is shown in Fig. 7 along with the resulting backscattered patterns taken at 30-degree increments. In this case, the silicone-resin coating

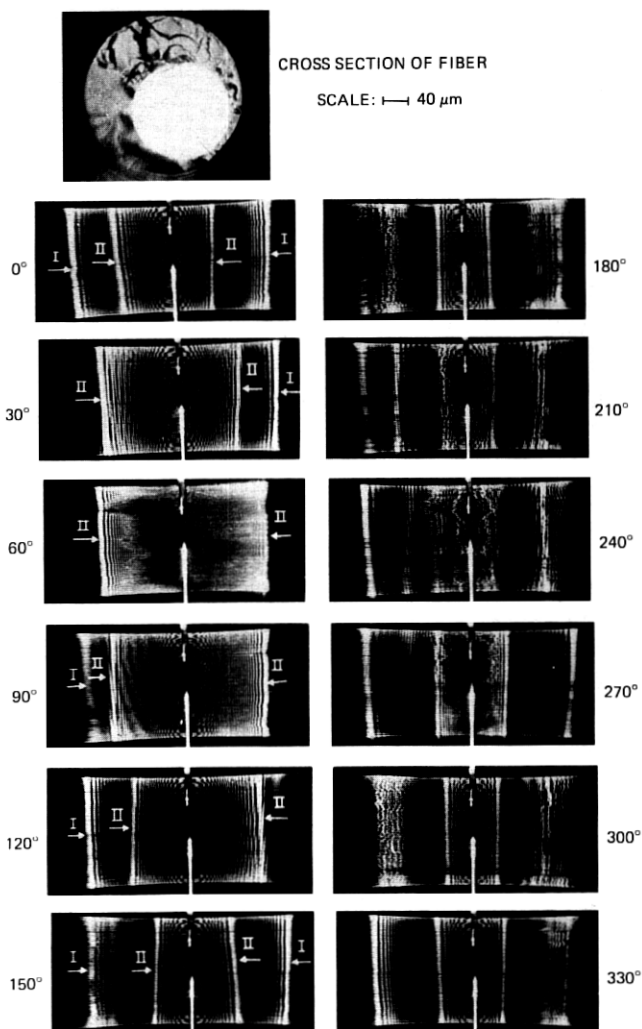
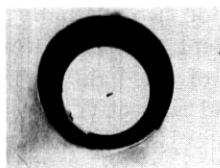


Fig. 6—Silicone-resin-coated fused-silica fiber with large nonconcentricity and associated backscattered patterns.



CROSS SECTION OF FIBER

SCALE:  $\text{---}$  40  $\mu\text{m}$

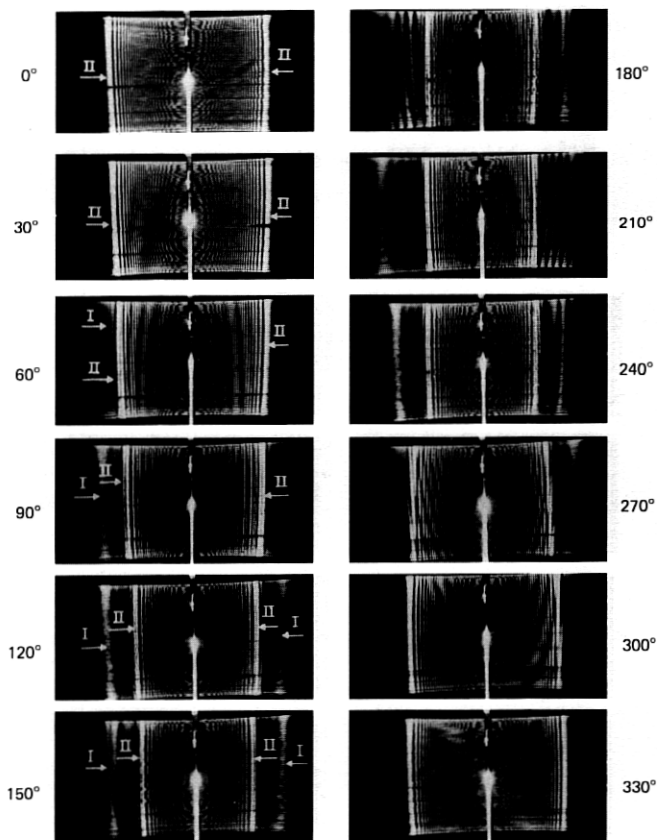
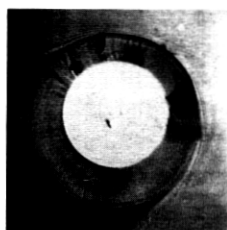


Fig. 7—Silicone-resin-coated fused silica fiber with coating thickness varying from 24  $\mu\text{m}$  to 52  $\mu\text{m}$  and associated backscattered patterns.

on the approximately 145- $\mu\text{m}$ -diameter fiber varies in thickness from 24  $\mu\text{m}$  to 52  $\mu\text{m}$ . The fringes arising from rays I and II are labeled in the 0- to 150-degree orientations. The light distributions exhibit considerably fewer variations compared with the previous fiber. Visual observations again are sufficient to detect nonconcentricity.

The silicone-resin coating on the optical fiber shown in Fig. 8 has a fair degree of concentricity, varying in thickness from approximately 45  $\mu\text{m}$  to 65  $\mu\text{m}$ . The backscattered light patterns shown in the same





CROSS SECTION OF FIBER

SCALE:  $\text{I} \rightarrow 60 \mu\text{m}$

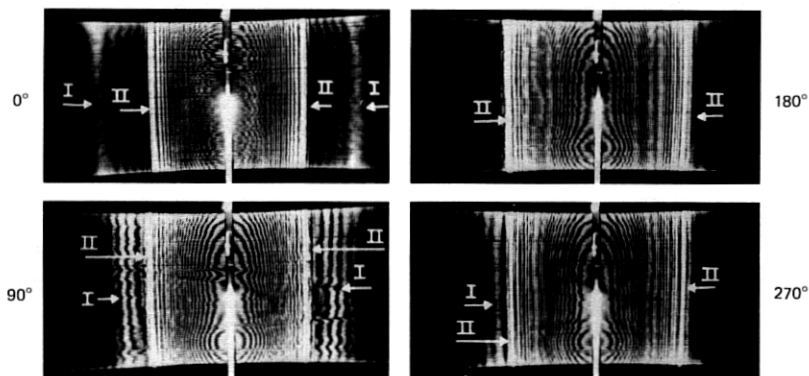


Fig. 8—Silicone-resin-coated fused-silica fiber with coating thickness varying from  $45 \mu\text{m}$  to  $65 \mu\text{m}$  and associated backscattered patterns at 90-degree increments. As in Figs. 6 and 7, a 6.5-cm length of fiber is illuminated.

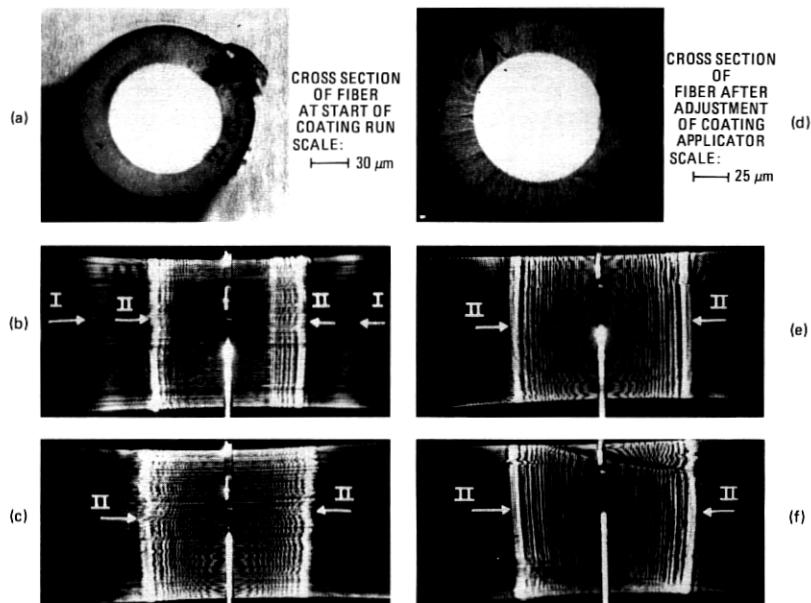


Fig. 9—On-line use of coating analyzer to improve concentricity.

figure were taken at 90-degree increments and indicate their sensitivity and ability to detect coating nonconcentricity from observations made in two perpendicular directions.

An example of the technique in use is afforded by the results in Fig. 9. The approximately 105- $\mu\text{m}$ -diameter glass fiber shown in Fig. 9a is a sample from the start of a silicone-resin-coating run. The coating thickness varies from 23  $\mu\text{m}$  to 36  $\mu\text{m}$ . This nonconcentricity is apparent in the two scattering patterns, Fig. 9b and c, taken at 90-degree orientations. After adjusting the coating applicator while observing the patterns for symmetry, as depicted by Fig. 9e and f, the coated-fiber sample appears as in Fig. 9d. The coating thickness now varies by less than 2  $\mu\text{m}$ , being about 28  $\mu\text{m}$  to 30  $\mu\text{m}$  thick.

The arrangement by which the real-time observations are made is depicted in Fig. 10. The beam from a 5-mW *He-Ne* laser, after being expanded in a manner similar to that of Fig. 5, strikes a beam splitter. A portion is transmitted directly to the fiber while the remainder, after reflections at the plane mirrors, impinges upon the fiber at right angles

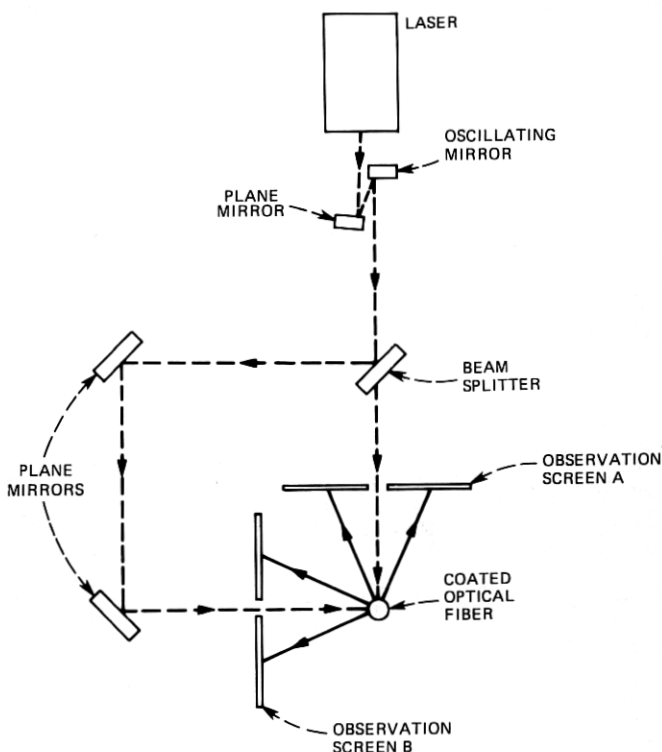
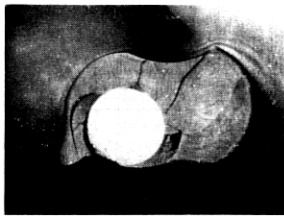


Fig. 10—Setup to monitor coating properties in on-line situation.



CROSS SECTION OF FIBER

SCALE:  $\longleftarrow \longrightarrow 40 \mu\text{m}$

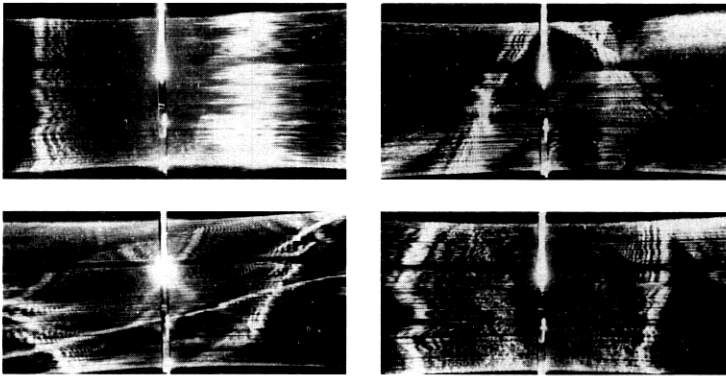


Fig. 11—Severely distorted plastic coating and associated backscattered-light patterns.

to the direct beam. The backscattered patterns are visually detected on two observation screens. Other components of the scattered light overlap the backscattered patterns, but due to their very different appearances, lower amplitudes and shifted locations present no problems.

The entire setup is mounted on a plate fastened to an  $x$ - $y$  positioner to allow real-time alignment with the fiber when necessary. The patterns are invariant to lateral motions of the fiber within the incident beams.<sup>10</sup> The position of the apparatus between the coating applicator and the take-up drum is determined by the coating state (before or after drying or curing) to be monitored. It is readily appreciated that the observation screen can be replaced or supplemented with detectors to automate the coating analysis.

In addition to observations of nonconcentricity, the technique is very sensitive to geometrical deformation and nonuniformities. Figure 11 shows a severely deformed silicone-resin-coated fiber along with some of its associated backscattered patterns. Such patterns indicate a problem and if corrective measures are not effective, the entire process can be stopped before more time and material were wasted.

The silicone-resin coating on the fiber shown in Fig. 12a appears to

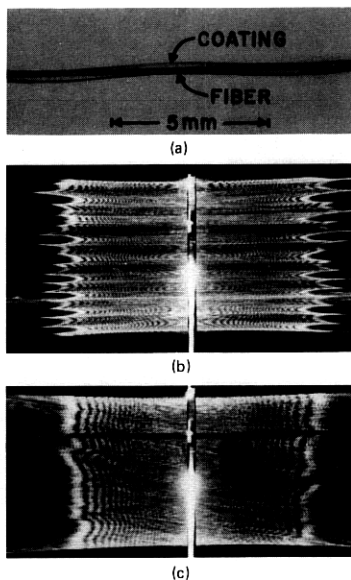


Fig. 12—Nonuniformly applied coatings and associated backscattered patterns. (a) and (b) Silicone resin. (c) Semitransparent polymer.

have been applied in some helical fashion. This is readily detected and observed in the associated scattering pattern, Fig. 12b.

The backscattered pattern of Fig. 12c arising from another coated fiber indicates a nonuniform coating. Despite the semicrystalline structure of the coating material applied to the fiber in this case, which renders it somewhat less transparent than silicone, the pattern is clear and can be used to analyze the coating.

#### IV. CONCLUSION

A sensitive, noncontacting, and nondestructive optical technique has been developed to evaluate the geometrical quality of plastic coatings on optical fibers both in laboratory and on-line situations. The method should prove valuable not only in analyzing coatings but also in developing the coating facilities themselves.

The technique has been applied to a variety, but not all, of the coatings currently under development. A necessary requirement for its implementation is that the coating material should be fairly transparent, a condition found satisfied by most of the plastic materials examined.

The theory of determining coating thickness is applicable only to the case of concentric coatings and should therefore be used with caution in other situations.

While visual observations have been emphasized, it would certainly be advantageous to automatically detect and electronically process the backscattered-light signal. This can be accomplished by known techniques utilizing photodiode arrays or vidicon scanning.

The method presented should also be applicable to extremely thick coatings as might be envisioned in fiber pigtail, jumper, or cabling operations and should aid in the production of uniform coatings in those areas as well.

## V. ACKNOWLEDGMENTS

The author would like to thank R. M. Derosier for the construction of the on-line coating-analysis apparatus, D. Marcuse for the computer calculations, and P. Kaiser for providing the fibers used in this study.

## REFERENCES

1. K. Yoshimura et al., "Low-Loss Plastic-Cladding Fibre," *Elect. Lett.*, *10*, No. 25/26 (December 12, 1974), pp. 534-535.
2. Y. Suzuki and H. Kashiwagi, "Polymer-Clad Fused-Silica Optical Fiber," *Appl. Opt.*, *13*, No. 1 (January 1974), pp. 1-2.
3. S. Tanaka et al., "Silicone-Clad Fused-Silica-Core Fibre," *Elect. Lett.*, *11*, No. 7 (April 3, 1975), pp. 153-154.
4. P. Kaiser, A. C. Hart, Jr., and L. L. Blyler, Jr., "Low-Loss FEP-Clad Silica Fibers," *Appl. Opt.*, *14*, No. 1 (January 1975), pp. 156-162.
5. L. L. Blyler, Jr. et al., "Low-Loss Silicone-Clad Fused Silica Fibers for Optical Communications," *Am. Ceram. Soc. Bull.*, *55*, No. 4, p. 455; Cincinnati Meeting, May 1-6, 1976, Paper 5-J1-76.
6. D. Gloge, "Optical Fiber Packaging and Its Influence On Fiber Straightness and Loss," *B.S.T.J.*, *54*, No. 2 (February 1975), pp. 245-262.
7. W. B. Gardner, "Microbending Loss in Optical Fibers," *B.S.T.J.*, *54*, No. 2 (February 1975), pp. 457-465.
8. C. R. Kurkjian et al. "Tensile Strength Measurements on Long Gage Lengths of Polymer-Coated Silica Fibers," *Am. Ceram. Soc. Bull.*, *55*, No. 4, p. 455; Cincinnati Meeting, May 1-6, 1976, Paper 8-J1-76.
9. A. H. Cherin and E. J. Murphy, "Quasi-Ray Analysis of Crosstalk Between Multimode Optical Fiber," *B.S.T.J.*, *54*, No. 1 (January 1975), pp. 17-45.
10. H. M. Presby, "Refractive Index and Diameter Measurements of Unclad Optical Fibers," *J. Opt. Soc. Am.*, *64*, No. 3 (March 1974), pp. 280-284.
11. H. M. Presby and D. Marcuse, "Refractive Index and Diameter Determinations of Step Index Optical Fibers and Preforms," *Appl. Opt.*, *13*, No. 2 (December 1974), pp. 2882-2885.
12. H. M. Presby, "Ellipticity Measurement of Optical Fibers," *Appl. Opt.*, *15*, No. 2 (February 1976), pp. 492-494.

